

Liquid Metal Nanoparticles as Initiators for Radical Polymerization of Vinyl Monomers

Jinwoo Ma,^{†,§,Ⓛ} Yiliang Lin,[†] Yong-Woo Kim,[§] Yeongun Ko,^{†,Ⓛ} Jongbeom Kim,[§] Kyu Hwan Oh,^{§,Ⓛ} Jeong-Yun Sun,^{§,Ⓛ} Christopher B. Gorman,^{‡,Ⓛ} Maxim A. Voinov,[‡] Alex I. Smirnov,[‡] Jan Genzer,^{†,Ⓛ} and Michael D. Dickey^{*,†,Ⓛ}

[†]Department of Chemical and Biomolecular Engineering, North Carolina State University, Raleigh, North Carolina 27695-7905, United States

[‡]Department of Chemistry, North Carolina State University, Raleigh, North Carolina 27695-8204, United States

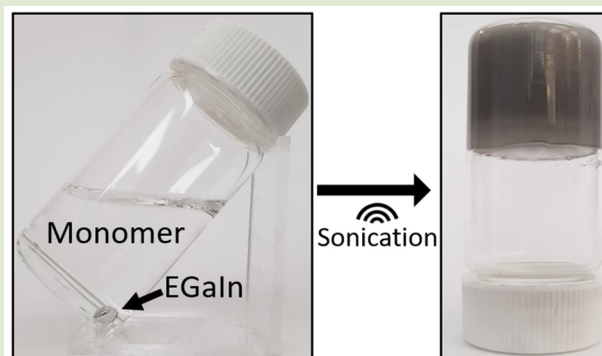
[§]Department of Material Science and Engineering, Seoul National University, Seoul 151-742, South Korea

[Ⓛ]Research Institute of Advanced Materials (RIAM), Seoul National University, Seoul 151-744, South Korea

Supporting Information

ABSTRACT: Sonication of gallium or gallium-based liquid metals in an aqueous solution of vinyl monomers leads to rapid free radical polymerization (FRP), without the need for conventional molecular initiators. Under ambient conditions, a passivating native oxide separates these metals from solution and renders the metal effectively inert. However, sonication generates liquid metal nanoparticles (LMNPs) of ~100 nm diameter and thereby increases the surface area of the metal. The exposed metal initiates polymerization, which proceeds via a FRP mechanism and yields high molecular weight polymers that can form physical gels. Spin trapping EPR reveals the generation of free radicals. Time-of-flight secondary ion mass spectrometry measurements confirm direct polymer bonding to gallium, verifying the formation of surface-anchored polymer grafts.

The grafted polymers can modify the interfacial properties, that is, the preference of the metal particles to disperse in aqueous versus organic phases. The polymer can also be degrafted and isolated from the particles using strong acid or base. The concept of physically disrupting passivated metal surfaces offers new routes for surface-initiated polymerization and has implications for surface modification, reduction reactions, and fabrication of mechanically responsive materials.



Many metals and metal alloys, including aluminum and stainless steel, readily form passivating native oxides at ambient conditions. Passivating oxide layers, typically a few nm thick, protect the reactive metals from further reactions. The ability to expose a metal surface to a reaction medium by stripping the protective oxide even temporarily might be advantageous for catalysis or redox reactions.^{1,2} Although surface oxides can be eliminated by etching³ or reduction,^{4,5} these oxides often reform rapidly and remain stable under ambient conditions; thus, it is desirable to find alternative ways to expose the metal to a reactive medium.

Gallium and several of its alloys (including eutectic gallium indium, EGaIn) possess low melting points,^{6–8} making it easy to disrupt mechanically the passivating oxide shell that forms on the surface of these liquids. Gallium's atomic configuration of $[\text{Ar}] 3d^{10}4s^24p^1$ is representative of odd electron species,^{9,10} making it a source of unpaired electrons that can potentially act as radical initiators for polymerization. Conventional radical polymerization, which is of great industrial relevance, is normally initiated by molecules that form free radicals via

homolytic bond cleavage in response to heat, light, or redox reaction.^{11–17} In this Letter, we show that sonication of small volumes of gallium and EGaIn can transiently rupture the passivating oxide and disperse the metal as liquid metal nanoparticles (LMNPs) with high surface areas. The exposed metal can initiate polymerization, which proceeds via a free radical polymerization (FRP) mechanism to form high molecular weight polymers grafted directly to the metal surface. The polymer can be degrafted and isolated by exposure to a strong acid or base. The grafted polymer overcoat dictates how the LMNPs disperse in water or organic solvents. The ability to modify the surface of LMNPs in a facile manner is noteworthy because of their functionality,^{18–24} facile formation,^{25–28} low toxicity,^{29,30} and applications including drug delivery,^{31–34} inkjet printing,³⁵ thermal interface materials,³⁶ and soft electronics.^{18,22,23,37}

Received: October 6, 2019

Accepted: October 28, 2019

Published: November 1, 2019

We initiated polymerization by sonicating gallium or eutectic gallium indium (EGaIn) in an aqueous solution of vinyl-based monomers such as acrylamide (AAM; vide infra). Under ambient conditions, both Ga and EGaIn form a passivating oxide on their surface.^{6–8} Sonication breaks the liquid metal into smaller particles (~ 100 nm in diameter, Figure S1) within minutes, thereby increasing the surface area of the metal to ~ 50 m²/g. Sonication of Ga or EGaIn in the presence of water-soluble, vinyl-based monomers results in polymerization and formation of a hydrogel, as shown in Figure 1. Sonicating

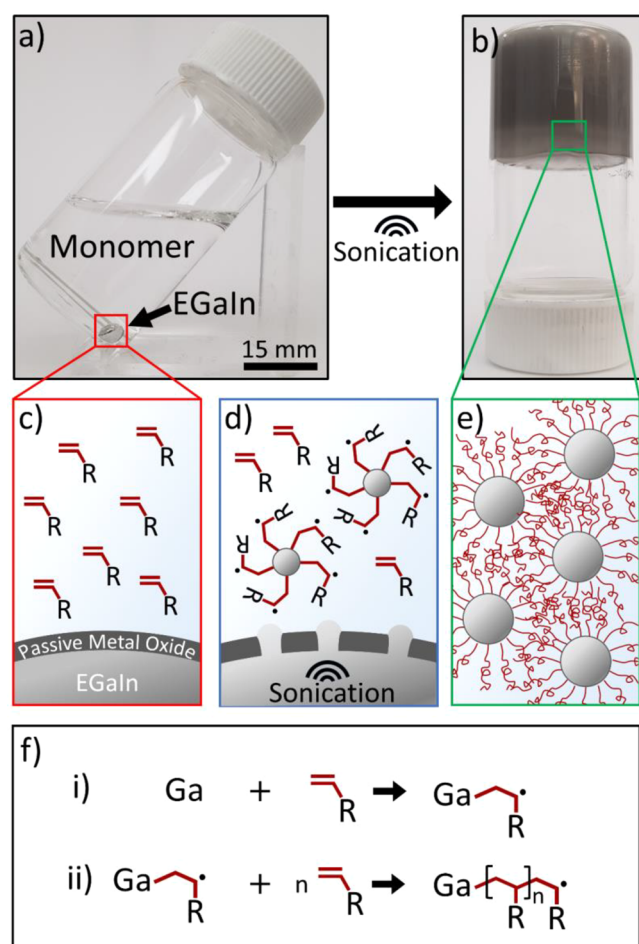


Figure 1. Liquid metal particles initiate free radical polymerization without the need for conventional molecular free-radical initiators. (a) A passivating oxide isolates the metal from the solution. Sonication breaks the liquid metal into small particles and thereby greatly increases surface area and exposes the metal, which initiates radical polymerization. (b) The resulting PAAm forms a physically cross-linked hydrogel. (c–e) Schematic illustration of the polymerization. (f) The suggested mechanism of initiation and chain growth.

monomer in the absence of Ga or EGaIn does not result in polymerization. The polymerization also occurs without any noticeable difference when the solution containing liquid metal and monomer was sparged with nitrogen. Although the LMNPs initiate polymerization of a variety of vinyl-based monomers (vide infra; Figure S2), we focus primarily on AAM.

For clarity, we first propose a FRP mechanism (Figure 1f) and then provide the evidence to support it. An unpaired electron from the gallium can react with the π -bond of the vinyl monomer. Thus, the polymerization initiates by the

formation of a covalent bond between gallium and carbon and proceeds through the generation of carbon-based free radicals that further react with nearby monomers.

Electron paramagnetic resonance (EPR) spin-trapping confirmed the formation of radical species in the reaction mixture. A water-soluble diamagnetic spin trap 5,5-dimethyl-1-pyrroline-*N*-oxide (DMPO) was added to the mixture of LMNPs and AAM in water 1 min after sonication. Figure 2a shows the EPR spectrum of the spin adduct(s) formed. The spectrum represents a superposition of spectra of at least two different types of radicals. The first, a weaker four-line spectrum (Figure 2a, spectral lines are marked with asterisks), shows 1:2:2:1 peak-to-peak intensity pattern with approximately equal interline splitting of 14.9 G. This is typical for the isotropic hyperfine couplings reported for DMPO–OH \cdot spin adduct ($A_N = A_H \approx 14.9$ G).³⁸ Another significantly stronger six-line pattern is characteristic of a DMPO adduct with a carbon-centered radical of the XCH₂–HC \cdot –Y general structure, where X = C or H and Y = electron-withdrawing substituent. The hyperfine coupling constants measured from the EPR spectrum ($A_N \approx 15.8$ G, $A_H \approx 22.8$ G, see Figure 2a) are similar to those reported for the DMPO adduct of CH₃–HC \cdot –OH radical.^{39,40} Thus, the observed six-line EPR spectrum corresponds most likely to the DMPO adduct with XCH₂–HC \cdot –CONH₂ radical, where X = C or H. This carbon-centered radical adduct does not form without AAM present. These results suggest that polymerization occurs via a free radical mechanism. We confirmed that the addition of hydroquinone, a radical scavenger, inhibited polymerization (Figures 2b and S3a–f). Replacing hydroquinone with diethyl hydroxylamine, another radical scavenger, also inhibited polymerization (Figure S3g).

To characterize the polymerization product, we degrafted the polymer by etching the surface of the LMNPs with NaOH solution (1 M, 5 min) and used centrifugation to separate the LMNPs from the polymer solution (Figure S4). The FT-IR spectrum of the polymer confirms the presence of polyacrylamide (PAAm; Figure 2c) and rules out the formation of polyamide-3 (an anionic polymerization is highly unlikely due to the presence of water).⁴¹ To confirm the polymerization of AAM we note that the C=C vibration band at 1610 cm^{–1} in AAM decreases with progressing AAM monomer conversion.⁴² The spectrum of the polymer is identical to PAAm prepared using a conventional thermally initiated bulk FRP using ammonium persulfate as an initiator (70 °C, 24 h).

¹H NMR further confirms the structure of PAAm. For the NMR characterization, as shown in Figure 2d, LMNPs were mixed with 0.5 M of AAM and glucono δ -lactone (GDL) in D₂O (Figure S5). Protons from hydrolyzed GDL slowly etch the oxide skin of LMNPs, exposing bare gallium to neighboring monomer molecules to promote FRP. There was no signal for LMNPs in the ¹H NMR spectrum (Figure S6a). The signals in the NMR spectrum correspond only to monomer, polymer, and the etchant. The signal of the etchant (~ 4 ppm) is distinct from the monomer or polymer (Figure S6). The characteristic peaks of PAAm in the ¹H NMR spectrum (methylene protons ~ 1.48 ppm and methine protons ~ 2.04 ppm) match well with those from a previous study.⁴³ FT-IR and ¹H NMR recorded after the polymerization of *N*-isopropylacrylamide (NIPAAm) using LMNPs initiator confirm the formation of poly(*N*-isopropylacrylamide) (PNIPAAm; Figure S7).

Water is the favorable solvent for the LMNP-initiated polymerization. Every water-soluble vinyl monomer we studied

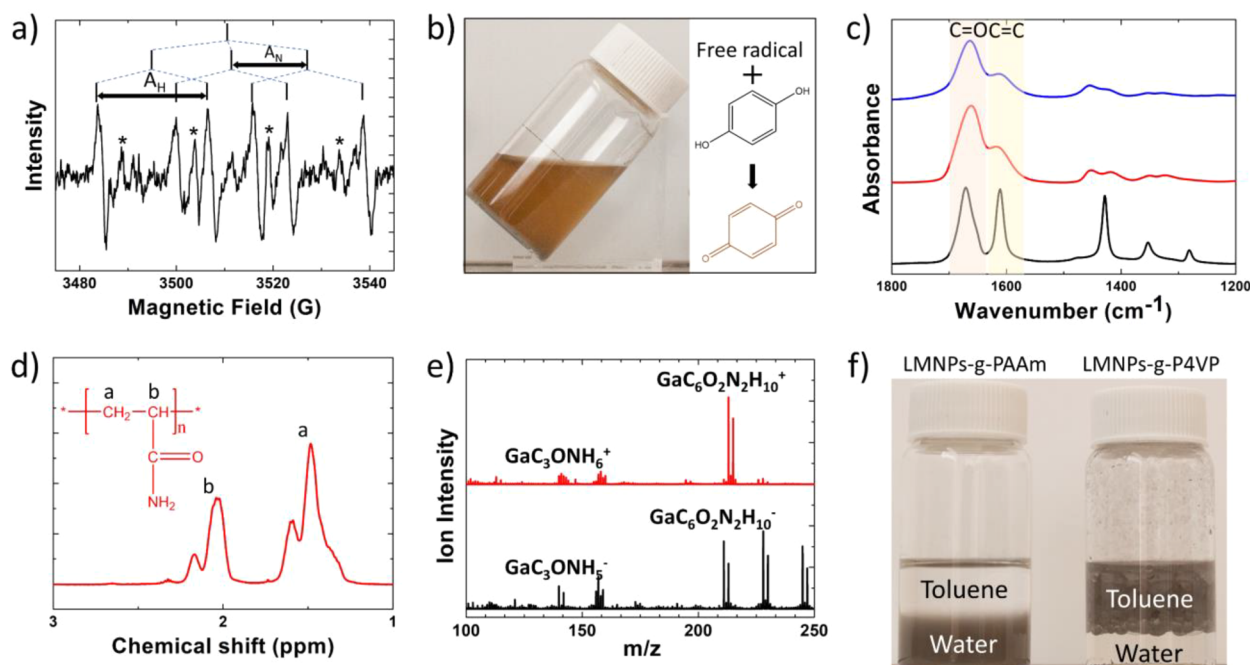


Figure 2. Evidence of free-radical polymerization initiated from the surface of LMNPs. (a) EPR spectrum of the spin adduct(s) of DMPO (100 mM) shows free radicals formed after sonication of an aqueous solution containing LMNPs and AAm. (b) A total of 0.1 g of EGaIn liquid metal was sonicated in the 4 M of AAm solution with hydroquinone present. Hydroquinone scavenged the free radicals, inhibiting polymerization and changing color to orange. (c) ATR FT-IR spectra of the powder of polymer degraded from LMNPs-polymer (blue), PAAm (red), and AAm monomer (black). (d) The ^1H NMR spectra (400 MHz, D_2O) illustrates that PAAm was formed from a solution of LMNPs (1 mg), AAm (0.5 M), and GDL (0.3 M). (e) TOF-SIMS spectra of the gallium-g-PAAm show Ga bonded directly to carbon from the monomer. (f) The polarity of the grafted polymers dictates how the LMNPs partition.

underwent polymerization (Figure S2). In addition, AAm polymerized in DMSO (dried by distillation), albeit at a slower rate than in water. 2-hydroxyethyl methacrylate (HEMA) also polymerized without water, and adding water did not noticeably affect the kinetics. Conversely, monomers that are not soluble in water (e.g., styrene) did not polymerize in organic solvents. These observations suggest that polar environments are important for the polymerization and that the presence of water might be critical for the polymerization, although the exact role of water remains unknown at this point.

The EPR spectrum in Figure 2a exhibits a pattern of small lines attributed to DMPO adducts of OH^\bullet radicals. These radicals have been employed previously to initiate polymerization via redox chemistry, the most well-known being the Fenton's reaction.⁴⁴ Although OH^\bullet radicals are capable of initiating polymerization, prior studies report the rates of the initiation to be slow, presumably due to the short-lived nature of these radicals.⁴⁵ For this reason, organo-peroxy radicals are often utilized to improve initiation rates. It is thus unlikely that OH^\bullet radicals initiate the polymerization. Instead, we propose gallium acts as an initiator for the polymerization.

If gallium directly initiates FRP, the growing polymer chains should be covalently attached to the metal. Previously, grafting of polymer on LMNPs has been accomplished by employing molecular initiators.⁴⁶ In contrast, the LMNPs act as the initiator in our study. The latter was confirmed by time-of-flight secondary ion mass spectroscopy (ToF-SIMS) experiment of LMNPs-g-PAAm (*g* refers to grafted). The spectra in Figure 2e and Table S1 show peaks with the masses corresponding to one ($m = 139.9621$ AMU) and two ($m = 227.9811$ AMU) AAm units attached to gallium. Each species has two peaks with an integrated area ratio of 3:2, as expected

given the two stable isotopes, ^{69}Ga and ^{71}Ga (68.9256 AMU and 70.9247 AMU, natural abundance 0.601 and 0.399, respectively). We also directly observed LMNPs and LMNPs-g-PAAm using transmission electron microscopy (TEM). The TEM images (Figure S8) show the presence of a PAAm halo (~ 20 nm thick) surrounding gallium nanoparticles when gallium was sonicated in the presence of AAm. In contrast, only an oxide skin (~ 3 nm thick) surrounds gallium nanoparticles in the absence of AAm. Taken in sum, the evidence provided here suggests that polymerization initiates from the surface of the particles, although we cannot fully rule out contributions of OH^\bullet radicals to polymerization.

A monomer added (after 3 h) to aqueous LMNP suspensions could still polymerize, albeit at a much slower rate compared to the monomer being present during sonication. Under these conditions, we did not observe any OH^\bullet radicals in solution by spin trapping EPR (not shown), which further suggests these species do not play a key role in polymerization. Particles created in the absence of monomer form surface oxide species. Nevertheless, polymerization may initiate on these particles based on the ability of electrons to tunnel through the relatively fresh (i.e., thinner) oxide according to Mott-Cabrera theory or due to the less passivating nature of oxides formed in water.^{47,48} Rheological measurements indicate that it takes 6 times longer to reach the gel point relative to the case when the monomer is present during sonication (Figure S9a,b).

The chemical composition of the grafted polymers on the LMNPs dictates how the particles partition between water and organic solvent phases.⁴⁹ To demonstrate this, we employed AAm to fabricate hydrophilic particles (LMNPs-g-PAAm) and 4-vinylpyridine (4VP) for organophilic particles (LMNPs-g-

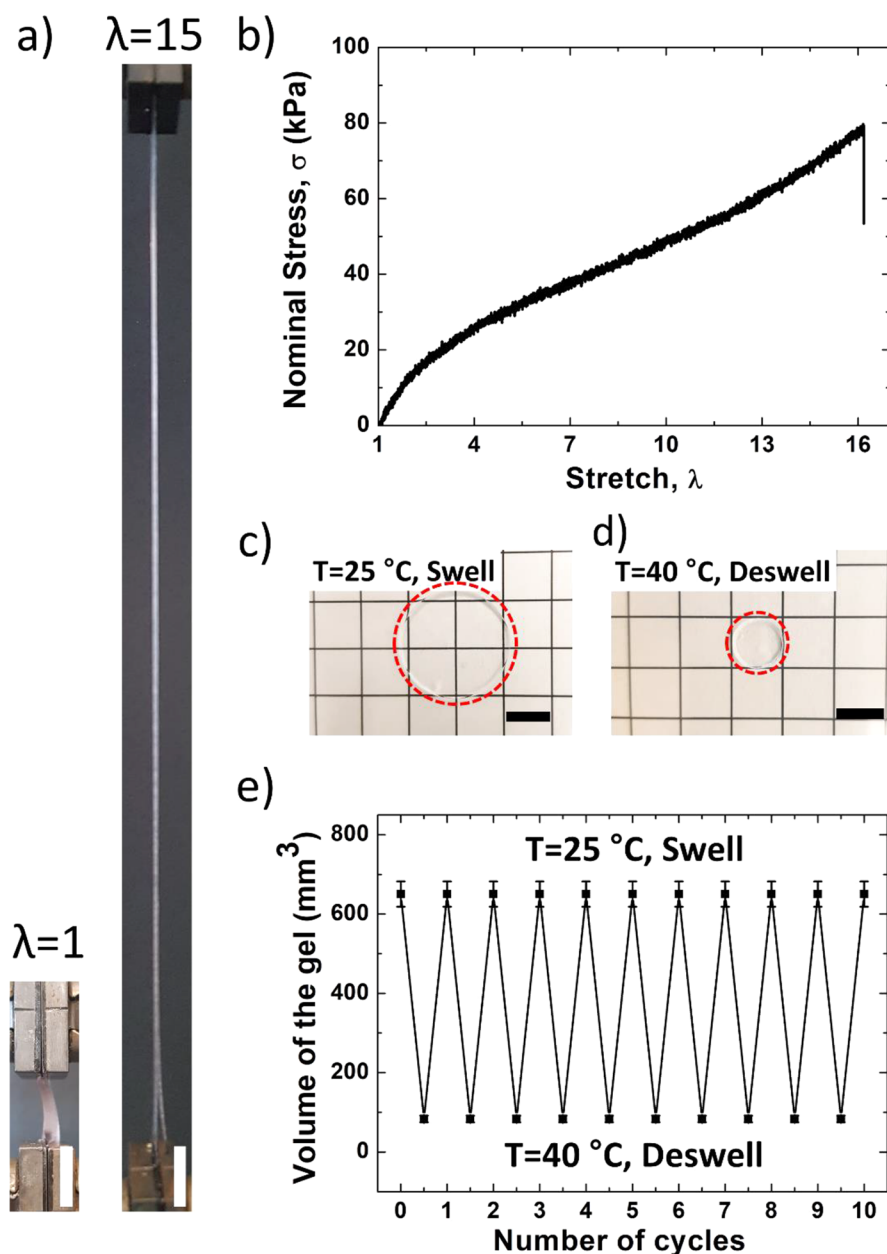


Figure 3. Synthesis of hydrogels using LMNPs as an initiator. (a) PAAm hydrogel synthesized by LMNP-based initiator, which showed high stretchability. Scale bar corresponds to 15 mm. (b) The stress–strain behavior of the hydrogel, showing a large strain at failure. (c, d) Temperature-responsive PNIPAAm hydrogel fabricated with LMNPs as an initiator. A hydrogel swells at 25 °C in deionized water (c) and a hydrogel fully deswells at 40 °C in deionized water. (d). The red dashed circles indicate the dimensions of the hydrogels. Scale bar corresponds to 10 mm. (e) Stable reversibility of the PNIPAAm hydrogel was confirmed by repeating the swelling–deswelling cycles.

P4VP) due to the insolubility of polymerized 4VP (i.e., P4VP) in water. We added toluene after the sonication and found that the LMNPs-g-PAAm suspends in the aqueous phase (Figure 2f, left). In contrast, the LMNPs-g-P4VP form a Pickering emulsion in the toluene phase due to the hydrophobicity of P4VP (Figure 2f, right), even after vigorous shaking. Similar partitioning was observed for other organic solvents, including those that are denser than water (Figure S10).

One would expect that the molecular weight of the polymer attached to the particles increases with increasing the monomer concentration in solution. To test this hypothesis, we precipitated LMNPs-g-PAAm suspensions in isopropyl alcohol and performed thermogravimetric analysis (TGA) in a nitrogen atmosphere. The mass of the polymer increased with

increasing monomer concentration (Figure S11). Assuming the same number of active initiator sites, the increased mass suggests a higher molecular weight of the polymers. We also tested whether the molecular weight of the polymer increased with the monomer concentration, which would be consistent with having a fixed number of initiating sites defined by the particle surface area. Unfortunately, the molecular weight of the PAAm was larger than the molecular weight cutoff of our size exclusion chromatography system (~ 1 MDa). Thus, although the molecular weight is likely greater than 1 MDa, we could not quantify the exact molecular weight of the polymers (Figure S12). Nevertheless, the elution speed increased with increasing monomer concentration, which is consistent with increasing the molecular weight of the polymer.

To demonstrate the applicability of the LMNPs, we prepared a highly stretchable PAAm hydrogel by including a N,N' -methylenebis(acrylamide) (MBAA) chemical cross-linker during sonication.^{50,51} As shown in Figure 3a,b, the hydrogel could stretch 15 times its original length. We also fabricated a PNIPAAm hydrogel that showed stable and reversible swelling/deswelling depending on the temperature of water (Figure 3c–e). Note that these samples are visually transparent despite the small amount of metal added as an initiator due to the addition of 0.1 g of GDL as a slow etchant for LMNPs. We also formed gels by pushing liquid metal and monomer between two syringes luer-locked together. The flow caused the metal to break up into relatively larger droplets (tens of microns in diameter). These droplets initiated polymerization, which suggests other mechanical routes of the initiation should be possible beyond sonication.

In summary, we show that sonicating bulk Ga or EGaIn generates liquid metal nanoparticles that initiate free radical polymerization of vinyl-based, water-soluble monomers, thus, leading to the production of high molecular weight hydrophilic polymers without the need for any conventional initiators. The method can yield highly stretchable PAAm and thermally responsive PNIPAAm hydrogels. The polymer can change the hydrophobicity of the LMNPs, yet it is also possible to degraft and isolate the polymer from the LMNPs by dissolving the particles. This simple approach constitutes the first example of free radical initiation using LMNPs, thus, presenting further opportunities toward novel methods for surface grafting as well as facile methods for synthesizing functional polymers and gels, including the use of mechano-induced chemistry.

■ ASSOCIATED CONTENT

Supporting Information

The Supporting Information is available free of charge on the ACS Publications website at DOI: 10.1021/acsmacrolett.9b00783.

The materials, the details describing polymer synthesis, the mechanical tests, EPR measurement, ToF-SIMS measurement, FT-IR spectroscopy, GPC measurement, TEM imaging, TGA characterization, ¹H NMR measurement, and rheological characterization of the gels (PDF)

■ AUTHOR INFORMATION

Corresponding Author

*E-mail: mddickey@ncsu.edu.

ORCID

Jinwoo Ma: 0000-0001-5140-2972

Yeongun Ko: 0000-0001-5770-6707

Jeong-Yun Sun: 0000-0002-7276-1947

Christopher B. Gorman: 0000-0001-7367-2965

Jan Genzer: 0000-0002-1633-238X

Michael D. Dickey: 0000-0003-1251-1871

Author Contributions

The manuscript was written through the contributions of all authors. All authors have given approval to the final version of the manuscript.

Notes

The authors declare no competing financial interest.

■ ACKNOWLEDGMENTS

J.M. is thankful to Dr. Junho Chung (SNU) for assisting with the interpretation of the NMR spectra. We thank Prof. David A. Shultz (NCSU) for helpful discussions. EPR instrumentation was supported by grants from the National Institutes of Health (no. RR023614), the National Science Foundation (no. CHE-0840501), and North Carolina Biotechnology Center (NCBC no. 2009-IDG-1015). Spin-trapping experiments were supported by the U.S. Department of Energy (DOE), Office of Science, Basic Energy Sciences (BES), under Award #DE-FG02-02ER15354. This research was a part of the project titled 'Development of cleanup technology for spilled oil and floating HNS using nanostructured structures', funded by the Korea Coast Guard of the Korean government. K.H.O. acknowledges the financial support of National Research Foundation (NRF-2016M3C1B5906481). M.D.D. acknowledges support of the National Science Foundation (CBET-1510772)

■ REFERENCES

- (1) Esrafilzadeh, D.; Zavabeti, A.; Jalili, R.; Atkin, P.; Choi, J.; Carey, B. J.; Brkljača, R.; O'Mullane, A. P.; Dickey, M. D.; Officer, D. L.; MacFarlane, D. R.; Daeneke, T.; Kalantar-Zadeh, K. Room temperature CO₂ reduction to solid carbon species on liquid metals featuring atomically thin ceria interfaces. *Nat. Commun.* **2019**, *10* (1), 865.
- (2) Gélin, P.; Primet, M. Complete oxidation of methane at low temperature over noble metal based catalysts: a review. *Appl. Catal., B* **2002**, *39* (1), 1–37.
- (3) Walker, P.; Tarn, W. H. *Handbook of Metal Etchants*; CRC Press, 1990.
- (4) Poizat, P.; Laruelle, S.; Grugeon, S.; Dupont, L.; Tarascon, J. M. Nano-sized transition-metal oxides as negative-electrode materials for lithium-ion batteries. *Nature* **2000**, *407* (6803), 496–499.
- (5) Morales, D.; Stoute, N. A.; Yu, Z.; Aspnes, D. E.; Dickey, M. D. Liquid gallium and the eutectic gallium indium (EGaIn) alloy: Dielectric functions from 1.24 to 3.1 eV by electrochemical reduction of surface oxides. *Appl. Phys. Lett.* **2016**, *109* (9), 091905.
- (6) Dickey, M. D. Emerging Applications of Liquid Metals Featuring Surface Oxides. *ACS Appl. Mater. Interfaces* **2014**, *6* (21), 18369–18379.
- (7) Daeneke, T.; Khoshmanesh, K.; Mahmood, N.; de Castro, I. A.; Esrafilzadeh, D.; Barrow, S. J.; Dickey, M. D.; Kalantar-zadeh, K. Liquid metals: fundamentals and applications in chemistry. *Chem. Soc. Rev.* **2018**, *47* (11), 4073–4111.
- (8) Dickey, M. D. Stretchable and Soft Electronics using Liquid Metals. *Adv. Mater.* **2017**, *29* (27), 1606425.
- (9) Robinson, G. H. Gallanes, Gallenes, Cyclogallenes, and Gallynes: Organometallic Chemistry about the Gallium–Gallium Bond. *Acc. Chem. Res.* **1999**, *32* (9), 773–782.
- (10) Fischer, R. A.; Weiß, J. Coordination Chemistry of Aluminum, Gallium, and Indium at Transition Metals. *Angew. Chem., Int. Ed.* **1999**, *38* (19), 2830–2850.
- (11) Sarac, A. S. Redox polymerization. *Prog. Polym. Sci.* **1999**, *24* (8), 1149–1204.
- (12) Chiefari, J.; Chong, Y. K.; Ercole, F.; Krstina, J.; Jeffery, J.; Le, T. P. T.; Mayadunne, R. T. A.; Meijs, G. F.; Moad, C. L.; Moad, G.; Rizzardo, E.; Thang, S. H. Living Free-Radical Polymerization by Reversible Addition-Fragmentation Chain Transfer: The RAFT Process. *Macromolecules* **1998**, *31* (16), 5559–5562.
- (13) Husseman, M.; Malmstrom, E. E.; McNamara, M.; Mate, M.; Mecerreyes, D.; Benoit, D. G.; Hedrick, J. L.; Minsky, P.; Huang, E.; Russell, T. P.; Hawker, C. J. Controlled Synthesis of Polymer Brushes by "Living" Free Radical Polymerization Techniques. *Macromolecules* **1999**, *32* (5), 1424–1431.
- (14) Yagci, Y.; Jockusch, S.; Turro, N. J. Photoinitiated Polymerization: Advances, Challenges, and Opportunities. *Macromolecules* **2010**, *43* (15), 6245–6260.

- (15) Hawker, C. J. Molecular Weight Control by a "Living" Free-Radical Polymerization Process. *J. Am. Chem. Soc.* **1994**, *116* (24), 11185–11186.
- (16) Decker, C. Photoinitiated crosslinking polymerisation. *Prog. Polym. Sci.* **1996**, *21* (4), 593–650.
- (17) Beuermann, S.; Buback, M. Rate coefficients of free-radical polymerization deduced from pulsed laser experiments. *Prog. Polym. Sci.* **2002**, *27* (2), 191–254.
- (18) Lin, Y. L.; Cooper, C.; Wang, M.; Adams, J. J.; Genzer, J.; Dickey, M. D. Handwritten, Soft Circuit Boards and Antennas Using Liquid Metal Nanoparticles. *Small* **2015**, *11* (48), 6397–6403.
- (19) Wu, Y.; Huang, L.; Huang, X.; Guo, X.; Liu, D.; Zheng, D.; Zhang, X.; Ren, R.; Qu, D.; Chen, J. A room-temperature liquid metal-based self-healing anode for lithium-ion batteries with an ultralong cycle life. *Energy Environ. Sci.* **2017**, *10* (8), 1854–1861.
- (20) Boley, J. W.; White, E. L.; Kramer, R. K. Mechanically sintered gallium-indium nanoparticles. *Adv. Mater.* **2015**, *27* (14), 2355–2360.
- (21) Kazem, N.; Hellebrekers, T.; Majidi, C. Soft Multifunctional Composites and Emulsions with Liquid Metals. *Adv. Mater.* **2017**, *29* (27), 1605985.
- (22) Pan, C.; Markvicka, E. J.; Malakooti, M. H.; Yan, J.; Hu, L.; Matyjaszewski, K.; Majidi, C. A Liquid-Metal–Elastomer Nanocomposite for Stretchable Dielectric Materials. *Adv. Mater.* **2019**, *31* (23), 1900663.
- (23) Liu, S.; Yuen, M. C.; White, E. L.; Boley, J. W.; Deng, B.; Cheng, G. J.; Kramer-Bottiglio, R. Laser Sintering of Liquid Metal Nanoparticles for Scalable Manufacturing of Soft and Flexible Electronics. *ACS Appl. Mater. Interfaces* **2018**, *10* (33), 28232–28241.
- (24) Farrell, Z. J.; Tabor, C. Control of Gallium Oxide Growth on Liquid Metal Eutectic Gallium/Indium Nanoparticles via Thiolation. *Langmuir* **2018**, *34* (1), 234–240.
- (25) Lin, Y.; Genzer, J.; Li, W.; Qiao, R.; Dickey, M. D.; Tang, S.-Y. Sonication-enabled rapid production of stable liquid metal nanoparticles grafted with poly(1-octadecene-alt-maleic anhydride) in aqueous solutions. *Nanoscale* **2018**, *10* (42), 19871–19878.
- (26) Yamaguchi, A.; Mashima, Y.; Iyoda, T. Reversible Size Control of Liquid-Metal Nanoparticles under Ultrasonication. *Angew. Chem., Int. Ed.* **2015**, *54* (43), 12809–12813.
- (27) Tevis, I. D.; Newcomb, L. B.; Thuo, M. Synthesis of liquid core-shell particles and solid patchy multicomponent particles by shearing liquids into complex particles (SLICE). *Langmuir* **2014**, *30* (47), 14308–14313.
- (28) Hohman, J. N.; Kim, M.; Wadsworth, G. A.; Bednar, H. R.; Jiang, J.; LeThai, M. A.; Weiss, P. S. Directing substrate morphology via self-assembly: ligand-mediated scission of gallium-indium microspheres to the nanoscale. *Nano Lett.* **2011**, *11* (12), 5104–5110.
- (29) Ivanoff, C. S.; Ivanoff, A. E.; Hottel, T. L. Gallium poisoning: a rare case report. *Food Chem. Toxicol.* **2012**, *50* (2), 212–215.
- (30) Kim, J.-H.; Kim, S.; So, J.-H.; Kim, K.; Koo, H.-J. Cytotoxicity of Gallium-Indium Liquid Metal in an Aqueous Environment. *ACS Appl. Mater. Interfaces* **2018**, *10* (20), 17448–17454.
- (31) Lu, Y.; Hu, Q.; Lin, Y.; Pacardo, D. B.; Wang, C.; Sun, W.; Ligler, F. S.; Dickey, M. D.; Gu, Z. Transformable liquid-metal nanomedicine. *Nat. Commun.* **2015**, *6*, 10066.
- (32) Yan, J.; Lu, Y.; Chen, G.; Yang, M.; Gu, Z. Advances in liquid metals for biomedical applications. *Chem. Soc. Rev.* **2018**, *47* (8), 2518–2533.
- (33) Chechetka, S. A.; Yu, Y.; Zhen, X.; Pramanik, M.; Pu, K.; Miyako, E. Light-driven liquid metal nanotransformers for biomedical theranostics. *Nat. Commun.* **2017**, *8*, 15432.
- (34) Tang, S.-Y.; Qiao, R.; Yan, S.; Yuan, D.; Zhao, Q.; Yun, G.; Davis, T. P.; Li, W. Microfluidic Mass Production of Stabilized and Stealthy Liquid Metal Nanoparticles. *Small* **2018**, *14* (21), 1800118.
- (35) Li, X.; Li, M.; Zong, L.; Wu, X.; You, J.; Du, P.; Li, C. Liquid Metal Droplets Wrapped with Polysaccharide Microgel as Biocompatible Aqueous Ink for Flexible Conductive Devices. *Adv. Funct. Mater.* **2018**, *28* (39), 1804197.
- (36) Bartlett, M. D.; Kazem, N.; Powell-Palm, M. J.; Huang, X.; Sun, W.; Malen, J. A.; Majidi, C. High thermal conductivity in soft elastomers with elongated liquid metal inclusions. *Proc. Natl. Acad. Sci. U. S. A.* **2017**, *114* (9), 2143.
- (37) Markvicka, E. J.; Bartlett, M. D.; Huang, X.; Majidi, C. An autonomously electrically self-healing liquid metal-elastomer composite for robust soft-matter robotics and electronics. *Nat. Mater.* **2018**, *17* (7), 618–624.
- (38) Minotti, G.; Aust, S. D. The requirement for iron(III) in the initiation of lipid peroxidation by iron (II) and hydrogen peroxide. *J. Biol. Chem.* **1987**, *262* (3), 1098–1104.
- (39) Chamulitrat, W.; Takahashi, N.; Mason, R. P. Peroxyl, alkoxy, and carbon-centered radical formation from organic hydroperoxides by chloroperoxidase. *J. Biol. Chem.* **1989**, *264* (14), 7889–7899.
- (40) Buettner, G. R. Spin trapping: ESR parameters of spin adducts. *Free Radical Biol. Med.* **1987**, *3* (4), 259–303.
- (41) Bhadani, S. N.; Prasad, Y. K. Simultaneous anodic and cathodic polymerizations of acrylamide. *Makromol. Chem.* **1977**, *178* (6), 1841–1851.
- (42) Jonathan, N. The infrared and Raman spectra and structure of acrylamide. *J. Mol. Spectrosc.* **1961**, *6*, 205–214.
- (43) Nieto, J. L.; Baselga, J.; Hernandez-Fuentes, I.; Llorente, M. A.; Piérola, I. F. Polyacrylamide networks. Kinetic and structural studies by high field ¹H-NMR with polymerization in situ. *Eur. Polym. J.* **1987**, *23* (7), 551–555.
- (44) Reyhani, A.; McKenzie, T. G.; Fu, Q.; Qiao, G. G. Fenton-Chemistry-Mediated Radical Polymerization. *Macromol. Rapid Commun.* **2019**, *40*, 1900220.
- (45) Nandi, U. S.; Palit, S. R. Hydrogen peroxide as initiator in vinyl polymerization in homogeneous system. I. Kinetic studies. *J. Polym. Sci.* **1955**, *17* (83), 65–78.
- (46) Yan, J.; Malakooti, M. H.; Lu, Z.; Wang, Z.; Kazem, N.; Pan, C.; Bockstaller, M. R.; Majidi, C.; Matyjaszewski, K. Solution processable liquid metal nanodroplets by surface-initiated atom transfer radical polymerization. *Nat. Nanotechnol.* **2019**, *14* (7), 684–690.
- (47) Cabrera, N.; Mott, N. F. Theory of the oxidation of metals. *Rep. Prog. Phys.* **1949**, *12* (1), 163.
- (48) Khan, M. R.; Trlica, C.; So, J.-H.; Valeri, M.; Dickey, M. D. Influence of Water on the Interfacial Behavior of Gallium Liquid Metal Alloys. *ACS Appl. Mater. Interfaces* **2014**, *6* (24), 22467–22473.
- (49) Barthet, C.; Hickey, A. J.; Cairns, D. B.; Armes, S. P. Synthesis of Novel Polymer–Silica Colloidal Nanocomposites via Free-Radical Polymerization of Vinyl Monomers. *Adv. Mater.* **1999**, *11* (5), 408–410.
- (50) Ma, J.; Lee, J.; Han, S. S.; Oh, K. H.; Nam, K. T.; Sun, J.-Y. Highly Stretchable and Notch-Insensitive Hydrogel Based on Polyacrylamide and Milk Protein. *ACS Appl. Mater. Interfaces* **2016**, *8* (43), 29220–29226.
- (51) Sun, J.-Y.; Zhao, X.; Illeperuma, W. R. K.; Chaudhuri, O.; Oh, K. H.; Mooney, D. J.; Vlassak, J. J.; Suo, Z. Highly stretchable and tough hydrogels. *Nature* **2012**, *489*, 133.